Journal of the Serbian Society for Computational Mechanics / Vol. 5 / No. 2, 2011 / pp. 129-146

(UCD: 616.13-004:004.925.84)

ARTREAT project: computer, experimental and clinical analysis of three-dimensional plaque formation and progression in arteries

N. Filipovic[1,2], M. Rosic[1], V. Isailovic[2], Z. Milosevic[2], D. Nikolic[2], D. Milasinovic[2], M.Radovic[2], B. Stojanovic[1], M. Ivanovic[1], I. Tanaskovic[1], I. Saveljic[2], M. Milosevic[2], D.Petrovic[2], M. Obradovic[1], E. Themis[3],A. Sakellarios[3], P. Siogkas[3], P. Marraccini[6], F.Vozzi[6], N. Meunier[4], Z. Teng[5], D. Fotiadis[3],O. Parodi[6], M. Kojic[2,7]

[1]University of Kragujevac, Kragujevac, Serbia, fica@kg.ac.rs
[2]Metropolitan University Belgrade - R&D Center for Bioengineering, BioIRC, Serbia
[3]University of Ioannina, Ioannina, Greece
[4]University Paris Descartes, Paris, France
[5]University of Cambridge, Cambridge, Great Britain
[6]National Research Council Pisa, Italy
[7]The Methodist Hospital Research Institute, Houston, USA

Abstract

Atherosclerosis is a progressive disease characterized by inflammation, monocyte-macrophage migration, and lipid accumulation in the vascular wall. Atherosclerosis is initially characterized by endothelial dysfunction, which favors lipid and cell elements crossing inside blood vessel wall.

In this study we investigated our three-dimensional computer model of plaque formation and development which we tested on experimental results obtained from rabbits and clinical study on human carotid and coronary arteries. Firstly, a model of plaque formation in the rabbit animal LDL transport model within simple experimental design is simulated numerically using animal data and histological recordings. Then some human patient data from carotid and coronary artery were used. The 3D blood flow is described by the Navier-Stokes equations, together with the continuity equation. Mass transfer within the blood lumen and through the arterial wall is coupled with the blood flow, and is modeled by a convection-diffusion equation. The LDL transports in lumen of the vessel and through the vessel tissue (which has a mass consumption term) are coupled by Kedem-Katchalsky equations. The inflammatory process is modeled using three additional reaction-diffusion partial differential equations. A full three-dimensional model was created. It includes blood flow and LDL concentration, as well as plaque formation and progression. From patient human carotid artery data we matched plaque volume progression using two and three time points for baseline, three and twelve months follow up. Also a group of patients with coronary artery disease (CAD) and intermediate lesions was evaluated by Computed Tomography Angiography (CTA), together with an innovative approach to simulate the WSS-related low density lipoprotein (LDL) transport across the endothelium and to identify LDL accumulation sites. The novelty of this work lies in the systematic verification of prediction of plaque progression by repeated CTA, six months after the baseline evaluation, and by patient-specific determinations of boundary conditions, including coronary vasodilating capability, known to affect local flow conditions. Our results for plaque localization correspond to low shear stress zone and we fitted parameters from our model using nonlinear least square method. Understanding and prediction of the evolution of

atherosclerotic plaques either into vulnerable or stable plaques are major tasks for the medical community.

Keywords: atherosclerosis, plaque formation and progression, computer modeling, finite element method, IVUS, histology

1. Introduction

Atherosclerosis is an inflammatory disease that starts with intima alterations. Over the past decade, scientists come to appreciate a prominent role of LDL for inflammation in atherosclerosis. Formerly focused on luminal narrowing due to the bulk of atheroma, the current concepts recognize the biological attributes of the atheroma as key determinants of its clinical significance [Libby P., 2002].

Inflammatory process starts with penetration of low density lipoproteins (LDL) in the intima. This penetration, if too high, is followed by leucocyte recruitment in the intima. This process may participate in formation of the fatty streak, the initial lesion of atherosclerosis and then in formation of a plaque [Loscalzo J. and Schafer A. I., 2003].

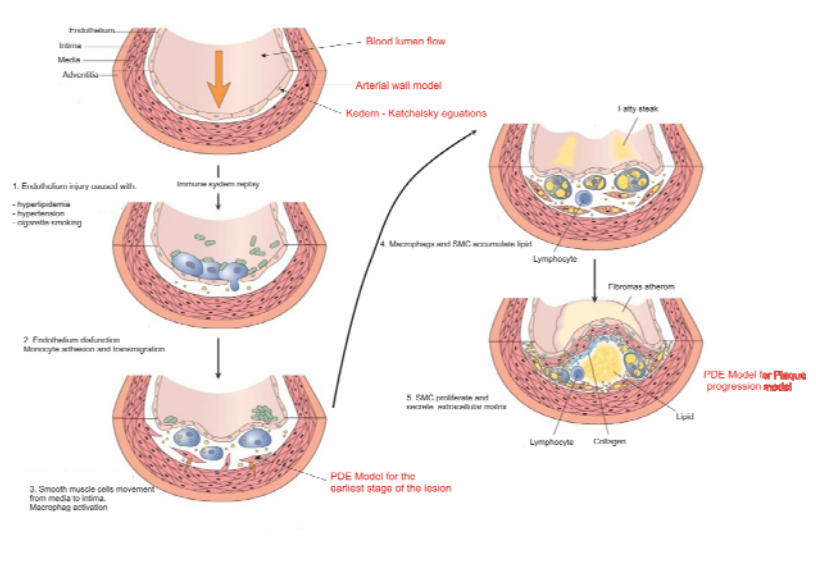

Fig. 1. Atherosclerotic plaque development (adapted from [Loscalzo J.and Schafer A. I., 2003])

Several mathematical models have recently been set up for the transport of macromolecules, such as low-density lipoproteins, from the arterial lumen to the arterial wall and inside the wall (*e.g.* [Tarbell, J. M., 2003 - Quarteroni A.et al, 2002.]). It is now well known that the early stage of the inflammatory disease is the result of interaction between plasma low density lipoproteins that filtrate through endothelium into the intima, cellular components (monocytes/macrophages, endothelial cells and smooth muscle cells) and the extracellular matrix of the arterial wall [Libby P., 2002 - Loscalzo J.and Schafer A. I., 2003],[Ross R., 1993].

In this study we describe computer model, experimental design and clinical study for 3D plaque formation and development. Computer model defines mass transport of LDL through the wall and a simplified inflammatory process, by coupling the Navier-Stokes equations, the Darcy equation for blood filtration and Kedem-Katchalsky equations [Kedem, O.and Katchalsky, A., 1961],[Kedem, O.and Katchalsky, A., 1958.] for the solute and flux exchanges between the lumen and intima. A system of three additional reaction-diffusion equations is formed for the inflammatory process and lesion growth in the intima.

Experimental design describes LDL mass transport and histological analysis of data. In the clinical study analysis, a group of patients with coronary artery disease (CAD) and intermediate lesions was evaluated by CTA, and an innovative approach was introduced to simulate the wall shear stress related LDL transport across the endothelium and to identify LDL accumulation sites.

Presentation of the basic equations is followed by results of modelling the plaque development in the rabbit experimental model, human carotid and coronary artery, discussion and concluding remarks.

2. Materials and methods

2.1. Computer model

We here summarize the fundamental equations for the LDL transport through blood vessel lumen and vessel wall, and for plaque development. The blood flow in lumen domain, considerd as a 3D fluid flow, is modeled by theNavier-Stokes equations, together with the continuity equation of incompressible fluid:

$$-\mu\nabla^2\mathbf{u}_l + \rho\left(\mathbf{u}_l\cdot\nabla\right)\mathbf{u}_l + \nabla p_l = 0 \tag{1}$$

$$\nabla\cdot\mathbf{u}_l = 0 \tag{2}$$

where $\boldsymbol{u_l}$ is blood velocity in the lumen, p_l is pressure, μ is the dynamic viscosity of blood, and ρ is blood density [Kojic M. et al, 2008.].

Mass transfer in the blood lumen is coupled with the blood flow and is modeled by a convection-diffusion equation,

$$\nabla\cdot\left(-D_l\nabla c_l + c_l\mathbf{u}_l\right) = 0 \tag{3}$$

in the fluid domain, where c_l is the solute concentration in the blood lumen, and D_l is the solute diffusivity in the lumen. Mass transfer in the arterial wall is coupled to the transmural flow and modeled by a convection-diffusion-reaction equation as follows

$$f\left(wss, c_l, generic\right) = \frac{\alpha_1\left(genetic\right)c_l}{1+\alpha_2 wss} \tag{4}$$

where c_w is the solute concentration and $D_w$is the solute diffusivity in the arterial wall; u_w is blood velocity in the wall, K is the solute lag coefficient, and $r_w$is the consumption rate constant. The LDL transports in lumen and in the vessel wall are coupled by the Kedem-Katchalsky equations:

$$J_v = L_p\left(\Delta p - \sigma_d\Delta\pi\right) \tag{5}$$

$$J_s = P\Delta c + \left(1-\sigma_f\right)J_v\overline{c} \tag{6}$$

where L_p is hydraulic conductivity of the endothelium; Δc is the solute concentration difference, Δp is the pressure drop and $\Delta\pi$ is the oncotic pressure difference, all across the endothelium; σ_d is the osmotic reflection coefficient, σ_f is the solvent reflection coefficient, P is the solute endothelial permeability, and $\overline{c}$ is the mean endothelial concentration. The first term in Kedem-Katchalsky equations $P\,\Delta c\,o$f the right hand side in (Eq 6) defines the diffusive flux across the endothelium, while the second term $\left(1-\sigma_f\right)J_v\overline{c}$ defines the convective flux. Only the oncotic pressure difference $\Delta\pi$ is neglected in our simulations because of decoupling the fluid dynamics from solute dynamics.

The above governing equations are transformed into a FE system of incremental-iterative equations and solved over time steps.

The atherosclerotic process starts with the accumulation of LDL in the intima, where part of them are oxidized and become pathological. In order to remove the oxidized particles, circulating immune cells (*e.g.* monocytes) are recruited. Once in the intima, the monocytes differentiate and become macrophages that phagocyte the oxidized LDL. Fatty macrophages then transform into foam cells. Foam cells are responsible for the growth of a subendothelial plaque which eventually emerges in the artery lumen.

The inflammatory process is modeled using three additional reaction-diffusion partial differential equations [Calvez V. et al, 2008],[Boynard M. et al, 2009]:

$$\begin{aligned}
&\partial_t Ox = d_1\Delta Ox - k_1 Ox\cdot M\\
&\partial_t M + div(v_w M) = d_2\Delta M - k_1 Ox\cdot M + S/(1+S)\\
&\partial_t S = d_3\Delta S - \lambda S + k_1 Ox\cdot M + \gamma(Ox - Ox^{thr})
\end{aligned} \tag{7}$$

where Ox is the oxidized LDL in the wall, M and S are concentrations in the intima of macrophages and cytokines, respectively; d_1,d_2,d_3 are the corresponding diffusion coefficients; λ and γ are degradation and LDL oxidized detection coefficients; and v_w is the inflammatory velocity of plaque growth, which satisfies Darcy's law and incompressibility continuity equation [Filipovic, N. et al, 2010]:

$$v_w - \nabla\cdot\left(p_w\right) = 0 \tag{8}$$

$$\nabla v_w = 0 \tag{9}$$

in the wall domain. Here, p_w is the pressure in the arterial wall.

In order to follow change of the vessel wall geometry during plaque growth, a 3D mesh moving algorithm ALE (Arbitrary Lagrangian Eulerian) is applied [Filipovic N. et al, 2006].

For plaque volume progression we need at least two points in time for different geometry where plaque growth can be observed from medical images. We use the following equations:

$$F_{t_{n(k+1)}}(i,j) = p_0(j) + p_1(j) * F_{t_{n(k)}}(i,j) + p_2(j) * \left.\frac{dF_{t_{n(k)}}(i,j)}{dt}\right|_{t_n} * \Delta t + p_3(j) * \left.\frac{d\tau^{wss}{}_{t_{n(k)}}(i,j)}{dt}\right|_{t_n} * \Delta t \tag{10}$$

where $F_{t_{n(k+1)}}(i,j)$ is a function of the coordinate or wall thickness *(i)* for cross section *(j)* at time t_n for iteration (*k*), *k=0,1,2,3…*; *n =1,2,3…* is time points for known image data from animal or human model. *p(0),p(1),…*are coefficients, τ^{wss} is wall shear stress Δt is time for each time step. Time derivatives of the functions are taken from the current known time step t_n and t_{n-1}. A

simple linear regression analysis with least square method is used for estimation of the coefficient *p(0), p(1)*… etc for each patient.

2.2. Experimental model of LDL transport on the rabbit animal data

Ex vivo blood vessels experiments of LDL transport were performed on the isolated rabbit a. carotis comm. All experiments were performed according to the Animals Scientific procedures Act 1986 (UK) and local ethical guidelines. New Zealand White rabbits of both sex weighing 3.5-4 kg were anesthetised using Ketamine (Laboratorio Sanderson, Santiago, Chile), 4-6 mg per kg of body weight. Blood vessel was excised and placed in the water bath. Cannulas with equally matched tip diameters (2mm) were mounted at proximal (cardial) and distal (cranial) ends of the blood vessel. The lumen was perfused with Krebs-Ringer physiological solution (KRS), using the peristaltic pump at 1 ml/min. The perfusate was continuously bubbled with a 95% O_2, and 5% CO_2 with the pH adjusted to 7,4 at 37 C. The distal cannula was connected to the resistance changing device. Perfusion pressure was measured with perfusion transducer (Fig.2).

The blood vessel was stretched to its approximate in vivo length. The outer diameter of the blood vessel was measured using digital camera and originally developed software. The blood vessel wall thickness was measured at the end of each experiment, using light microscope and microscopically graduated plate (see Fig. 3). The blood vessel was considered to be viable if it contracted when 25 mMKCl was added to the bath, as well as if the presence of functional endothelium was verified by dilation with Ach (1μM) at the end of experiment.

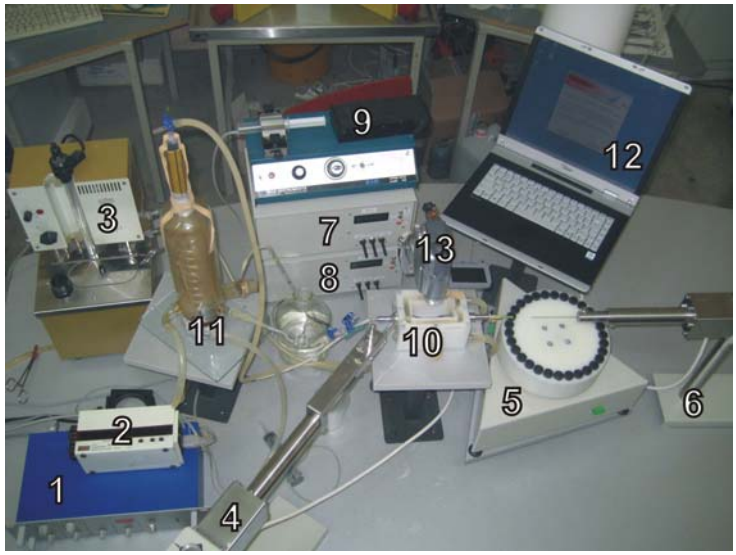

Fig. 2. Setting for *ex vivo* blood vessels experiments: 1. Pressure and temperature A/D converter, 2. Peristaltic pump, 3. Heater thermostat, 4. Rapid infusion pump (RIP), 5.Automatic sampler, 6. Resistance changing device (RCD), 7. Control unit for RIP, 8. Control unit for RCD, 9. Syringe infusion pump, 10. Water bath, 11. Heating stabiliser, 12. PC, 13. Digital camera.

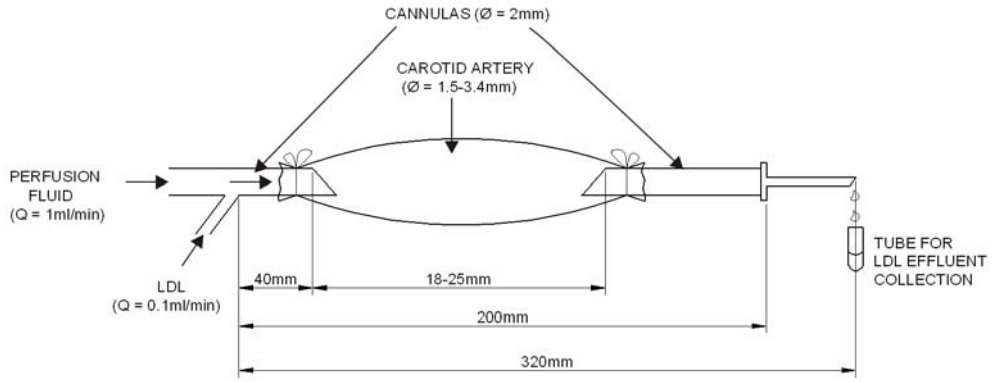

Fig. 3. Schematic presentation of the isolated blood vessel segment in the water bath

The isolated blood vessel was placed into the water bath with physiological buffer. After the equilibration period (20-30 min) at constant perfusion flow of 1 ml/min, 100μl bolus was injected into the perfusion system containing ^{99m}Tc-Nanocis as an intravascular marker (referent tracer), or ^{125}I-LDL as a test molecule. The first 15 samples (3 drops in each sample) and 9 cumulative 3 min samples of perfusion effluent were sequentially collected. All samples were prepared for measurement of ^{125}I-LDL specific activity by addition of physiological buffer until final volume of 3 ml/sample. Measurements of perfusion effluent samples containing ^{99m}Tc-Nanocis or ^{125}I-LDL were performed by means of the gamma counter (Wallac Wizard 1400).

The ^{125}I-LDL uptake is derived from the difference between the ^{99m}Tc-Nanocis value and that of ^{125}I-LDL recovery in each sample.

2.3. Clinical study analysis

Patients at intermediate risk for CAD admitted to CNR Clinical Physiology Institute - Fondazione Gabriele Monasterio of Pisa and in whom a coronary CTA demonstrated the presence of atherosclerosis lesions, confirmed by invasive coronary angiography, were enrolled. Also patients in whom potentially "vulnerable" coronary lesions were detected or had percutaneous coronary intervention with stent implantation were asked for participating to the study. In the enrolled patients, blood samples for determination of specific biomarkers linked to atherosclerotic process, were withdrawn at baseline and after 6 month follow-up. Inclusion criteria were: patients with a clinical indication to CTA according to the guidelines, with documented CAD by CTA confirmed by coronary angiography; evidence of one or more non-significant lesion; patient's informed consent. Exclusion criteria were: unstable clinical condition; heat failure or post-ischemic myocardial dysfunction (ejection fraction < 0.45); adverse reactions to contrast agents during the first coronary angiography; intolerance to adenosine administration; female with non-childbearing potential. Pharmacological therapy and lifestyle were optimized in all patients immediately after knowledge of CTA results. Each patient was informed about aim and risk of the procedures and signed a consent before study entry.The study protocol was approved by the local Ethics Committee.

3. Results

Firstly we examined LDL transport through animal model (rabbit carotid artery) under high blood pressure 140 mmHg and low perfusion flow 1.1ml/min.

The aim of our experiment was to determine distribution of accumulated ^{125}I-LDL radioactivity in the different segments of the isolated blood vessel. Specific software for 3D reconstruction of lumen domain and carotid wall artery was developed. Computer model of the artery is considered as a simple straight tube with deformation during high pressure of 140 mmHg. The diameter of artery was D=0.0029m, the mean velocity U_0=0.24m/s, dynamics viscosity μ=0.0035Pa s, density ρ=1050 kg/m^3.

Histological images are shown in Fig. 4. The labeled LDL is localized in the white zones inside media which is probably due to destroyed radioactive LDL of tissue. Polylines around media are segmentation lines produced by in-house image processing software. Matching of histological data and computational simulation is presented in Fig. 5. The process of matching histological images was done by 2D deformation of each histological cross-section in order to keep the internal lumen approximately be cylindrical shape. The maximum LDL was found at distal part of the carotid artery segment at 3.5 mm from entry segment which corresponds to the largest artery diameter. This finding correlates to well accepted research about the lowest shear stress influence. A full three-dimensional finite element analysis was performed using our in-house finite element code in order to connect the wall shear stress and function of permeability for the wall. Diagrams of wall LDL and oxidized LDL are shown in Fig. 6. Experimental LDL transport of 15.7% was fitted with specific nonlinear least square analysis, Chavent 2010 [Bourantas, C. et al, 2005] in order to get numerical parameters. The fitted numerical parameters are given in Table I.

TABLE I
VALUES FOR RABBIT CAROTID ARTERY EXPERIMENT

Lumen	**Intima**	**Inflammation**
ρ=1000 kg/m^3		d_1=10^{-7} m^2/s
μ = 0.035 [*P*]		d_2=10^{-7} m^2/s
D_l = 1.0e10^{-12} m^2/s	D_w= 3.0e^{-12} m^2/s	d_3=10^{-7} m^2/s
Umax=0.4m/s	r_w = -2.6x10^{-4}	k_1=1.9e^{-4} m^3/kg s
Pout=120mmHg	Pmed=100mmHg	λ=25 s^{-1}
Co=3.0x10^{-12} kg/m^3		γ = 1 s^{-1}

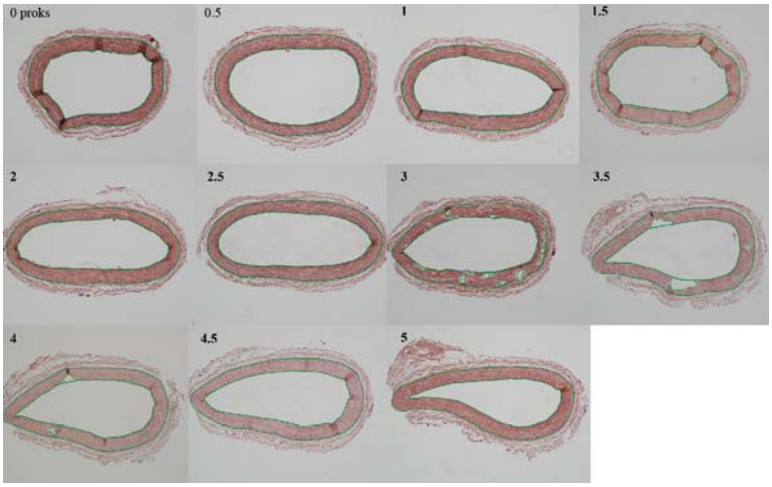

Fig. 4. Histological data (numbers on photos indicate distances from entry carotid artery in millimeters). White zones inside media denote labeled LDL localization. Polylines around media are segmentation lines produced by image processing software.

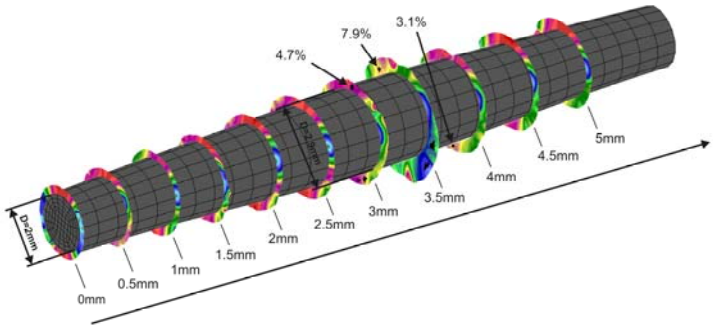

Fig. 5. Labeled LDL located in histological cross-sections on each 0.5 mm for a straight segment. Histological segments were obtained as deformable elastic rings opened from the current squeezed position to circular original tube. Black holes in these cross-sections show location of the labeled LDL. Percentages show labeled LDL area inside media and intima wall thickness.

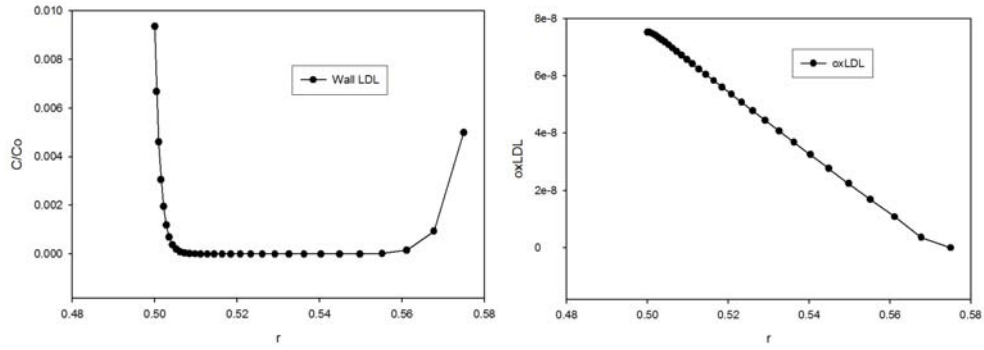

a) b)

Fig. 6. Computational results: a) Dimensionless wall LDL concentration profile in the media; b) Oxidized LDL concentration profile in the media, *r* is radial position at the cross section [mm]

a)

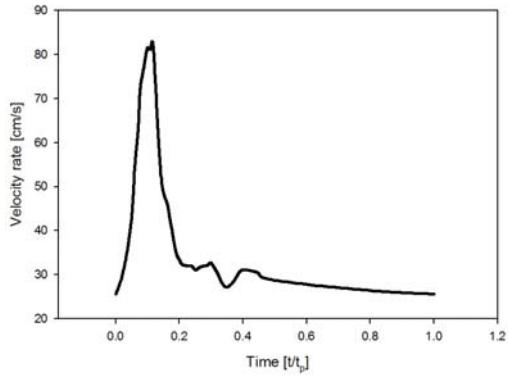

b)

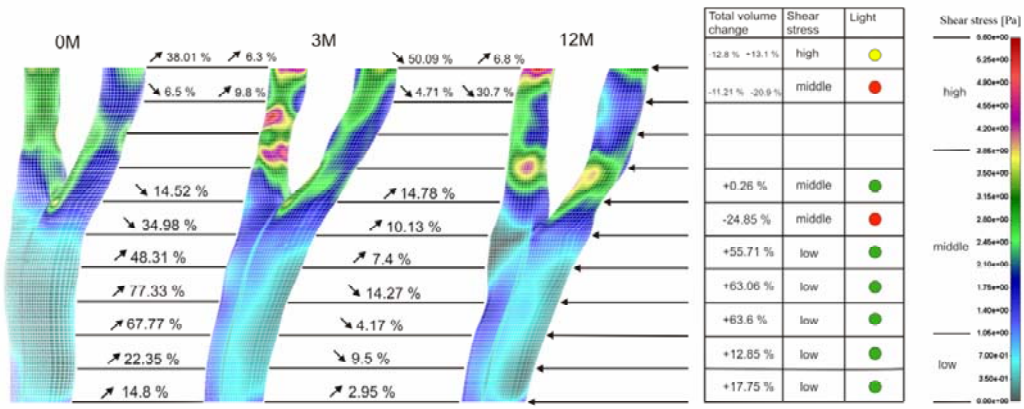

Fig. 7. Carotid artery simulation for a specific patient. a) Inlet velocity profile measurement from MRI at the common carotid artery; b) Correlation of cross-sections changes with wall shear stress

The next example is related to human carotid artery. We compared changes in the cross-section areas for different carotid artery patient from University of Cambridge partner in EU ARTreat project [ARTreat FP7-224297 EU project 2008-2011]. From 50 patients we choose a few with significant changes in the cross-sections area in order to find correlation with wall shear stress. Inlet velocity profile for baseline at the common carotid artery is presented in Fig. 7a. Different cross-section areas for zero, three and twelve months for a specific patient are presented in Fig. 7b. It can be seen that almost all cross-section areas are increasing in time. For a specific patient the correlation with wall shear stress zones is shown in Fig. 7b. We used three categories as colors for the light: red color denotes large decreasing in the cross-section area changes and middle wall shear stress, yellow color denotes small decreasing in the cross-section area changes and middle wall shear stress, while increasing in the cross-section area changes and low wall shear stress is shown by green color. Obviously, it can be concluded from Fig. 7b that there is a significant correlation with large increasing of the cross-section areas and low wall shear stress for this patient.

a)

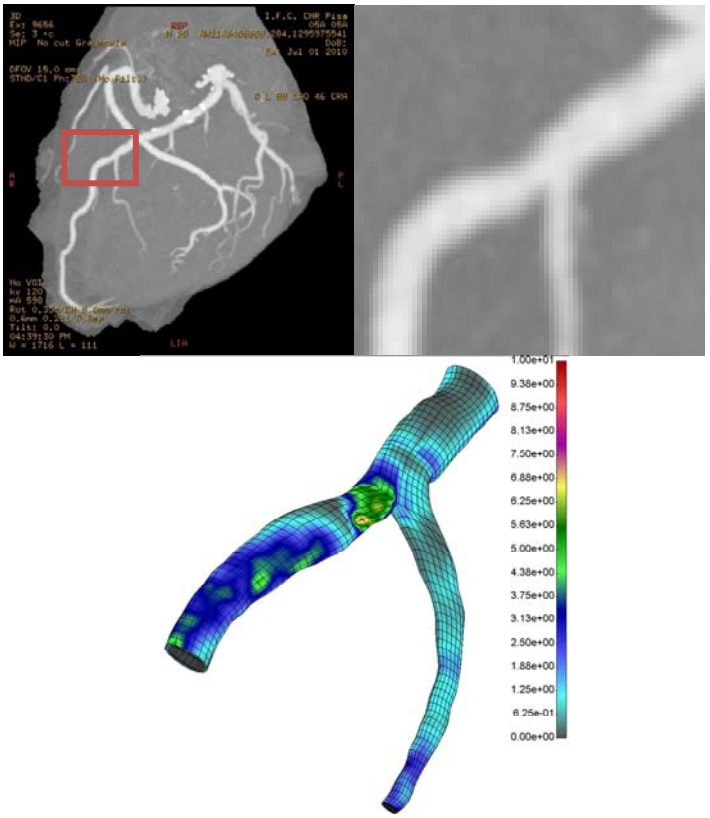

b)

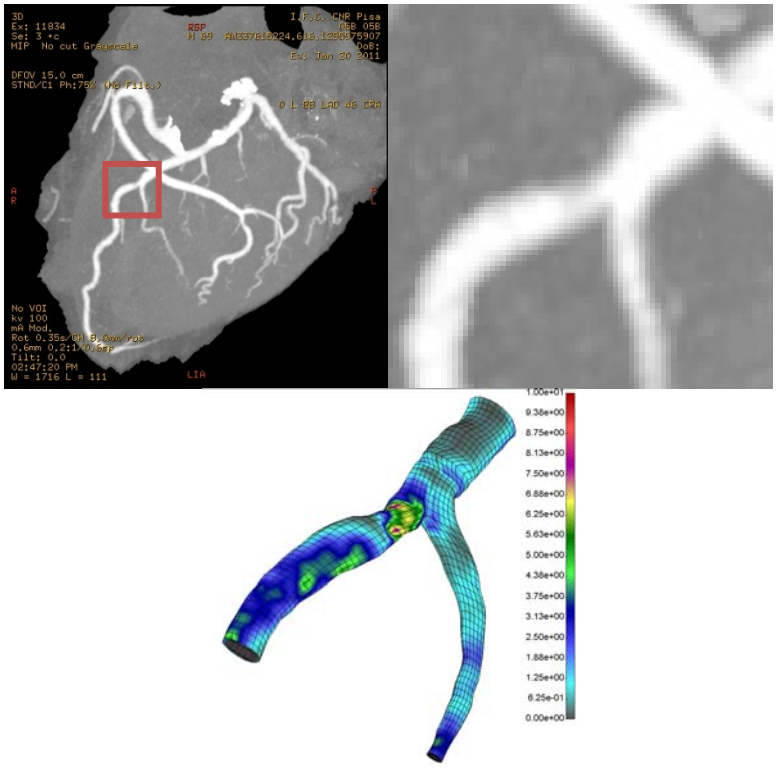

Fig. 8. LAD distal segment for patient angiography images and shear stress distribution. a) Baseline segment; b) Follow-up six months, plaque progress and volume increasing

The following example is from human data at CNR Pisa patient #5. It is LAD distal segment which was measured two times, at baseline and six months after that. There was a significant plaque progress which was indicated inside red box at upper and down left panels in Fig. 8. The low shear stress distribution corresponds to the location of the plaque progression.

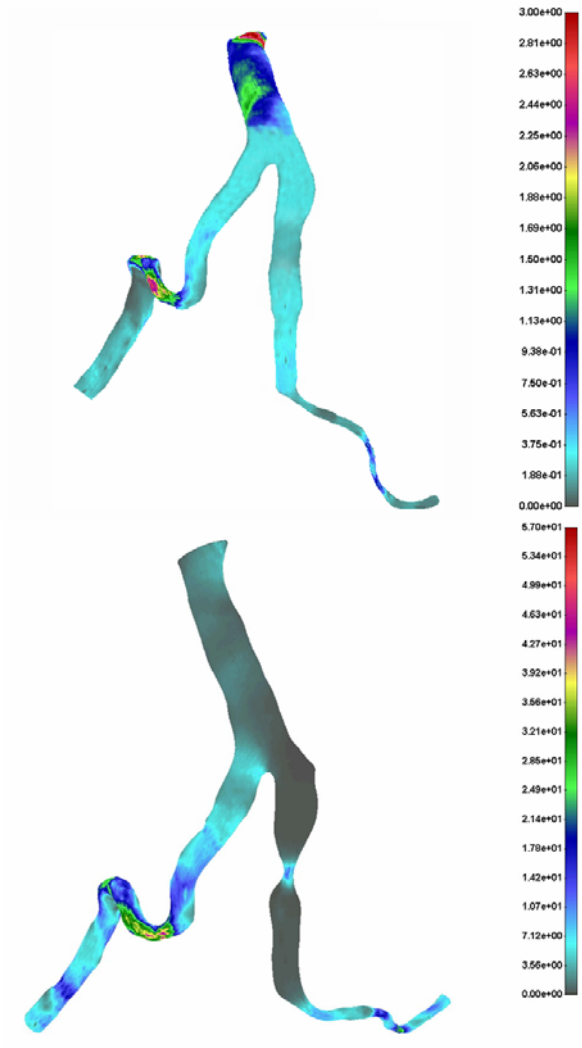

Fig. 9. Plaque progression for coronary artery at specific patient #5, shear stress distribution. a) Baseline; b) Follow up study after 6 months

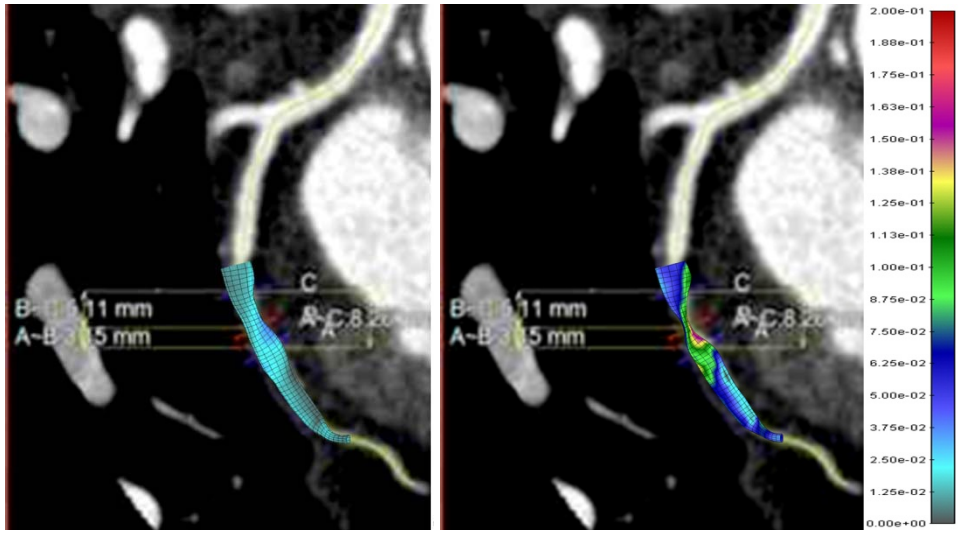

Fig. 10. LDL distribution for baseline and follow- up study after 6 months for coronary artery segment in the patient #5. Angiography slices are in the background of the computer simulation results. Units for LDL concentration [mg/ ml].

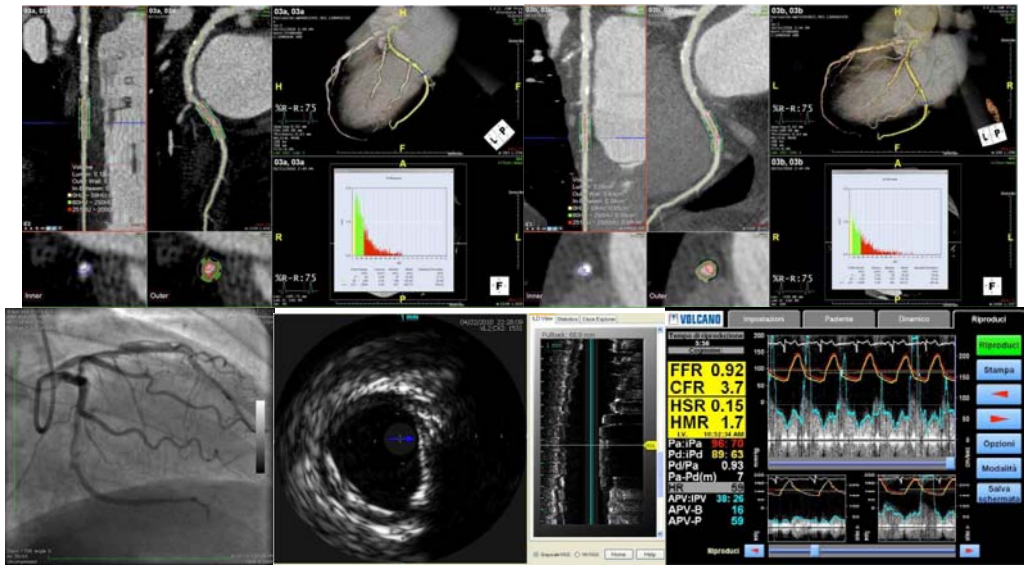

Fig. 11. Coronary CTA angiography at baseline and at 6 months (upper, left and right panels, respectively), 2D coronary angiography (lower panel, left), IVUS study at the level of distal CX lesion (lower panel, middle), pressure and Doppler flow velocity of the same CX segments (lower panel, right) in patient #3. CTA detects a non-obstructive (35% lumen diameter reduction) mixed plaque that progressed at 6 months (48% lumen diameter reduction). CFR was markedly reduced at baseline evaluation (1.7), indicating an impaired microcirculatory vasodilating capability.

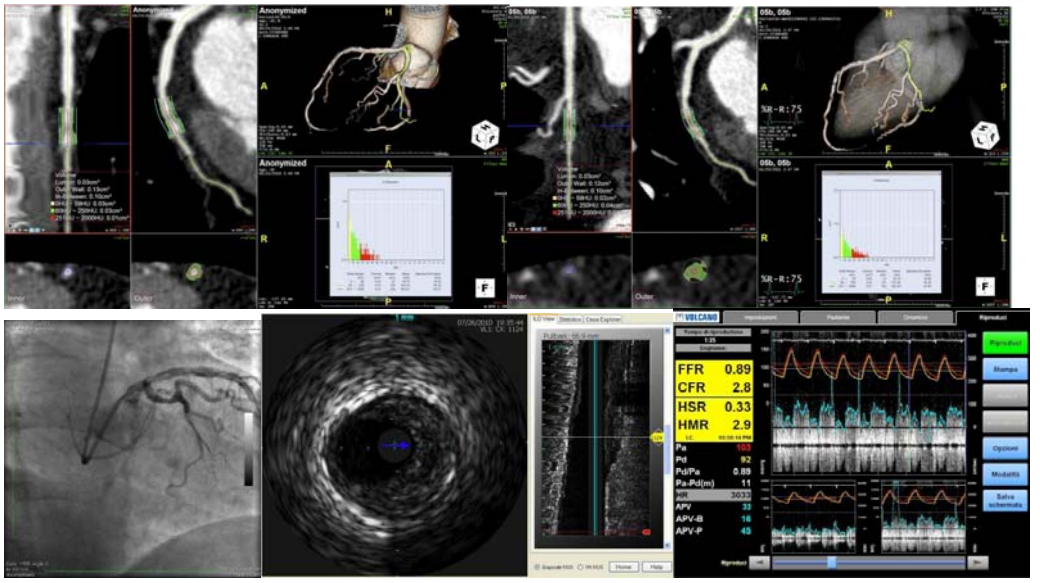

Fig. 12. Coronary CTA angiography at baseline and at 6 months (upper, left and right panels, respectively), 2D coronary angiography (lower panel, left), IVUS study at the level of distal CX lesion (lower panel, middle), pressure and Doppler flow velocity of the same CX segments (lower panel, right) in patient #5. CTA detects a non-obstructive (33% lumen diameter reduction) soft plaque that progressed to an almost critical stenosis at 6 months (67% lumen diameter reduction). CFR was almost normal, while FFR was reduced at baseline evaluation (0.84), indicating a slight hydraulic impact of the 2 CX lesions on the coronary flow.

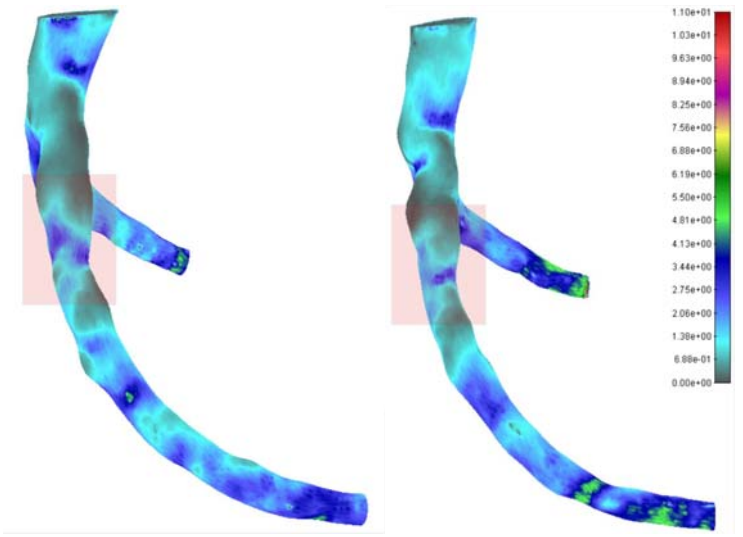

a) b)

Fig. 13. Shear stress distribution for baseline (a) and after 6 months follow up (b) for patient #3 (units [Pa])

Plaque progression for human coronary artery at two time points is also presented in Fig. 9. Shear stress distributions for baseline and follow up study after six months have been shown. It can be seen that low shear stress again is matched with the location of the plaque progression. That is only initial point for our simulation. Using nonlinear least square analysis [Chavent, Guy, 2010] we fitted all other parameters from eqs. 8,9. Fluid shear stress in our model is used for the plaque initiation and position at the wall for higher LDL penetration. Complex process of the macrophages transformation into the foam cells which is described with eqs. 5-7 in the Section 2. Also the foam cells directly created the intima volume increase which is described by eqs. 8-9. ALE formulation is developed for mesh moving and changing of the structural domain due intima volume thickness and fluid domain reducing in time. LDL distribution for baseline and follow-up study after 6 months has been shown in Fig. 10. It can be observed that after 6 months there is a significant increase in LDL distribution distal from the most narrowing part of the lumen domain. Due to complex lumen and wall domain only LDL distribution for the joint boundaries is presented in Fig. 10.

Four of the 10 enrolled patients completed the six month follow-up by CTA, following the baseline evaluation (patients #1, #3, #4, #5). CTA allowed a complete evaluation of the three main coronary arteries, with high quality visualization of vessel geometry and pathway, and a good definition of plaque characteristics. At baseline, IVUS and 2D coronary angiography permitted to confirm the presence of target lesions in all patients, with further details on plaque composition. Two out of the 4 patients showed an obvious reduction of lumen diameter, indicative of plaque progression, both in the distal portion of the circumflex artery. Plaque was defined mixed in one patient and soft in the other, according to CTA and IVUS criteria. Plaque progression occurred in a bend region of the vessel and in its inner part in both patients. CFR was within the normal range (> 3) in all investigated segments but one (CFR 1.7), corresponding to the circumflex artery with plaque progression (patient 3). FFR was within the normal values (> 0.92) in all investigated segments but one (FFR 0.84), located in the circumflex artery with the most obvious plaque progression (patient #5). Thus, the 2 segments with plaque growth at 6 months follow-up in patients #3 and #5 were characterized by impaired CFR or reduced FFR, respectively. Imaging and Doppler flow velocity data in the two patients with plaque progression are shown in Figs. 11-12.

In the distal portion of circumflex artery at the bifurcation level with the second marginal branch, predominantly low WSS values occur at baseline in patient #3 (Fig. 13a). High WSS values occur after 6 months follow up due the volume decreasing from the baseline lumen domain. This directly affects on the velocity distribution at vessel giving rise to higher WSS values. Furthermore, the WSS exhibits high values in the distal regions of the CX, where the magnitude of the mean flow velocity is relatively higher, due to vessel tapering (Fig. 13b).

4. Conclusions

We described inflammatory process by a reaction-diffusion PDE system. Our model starts with passive penetration of LDL in particular areas of the intima. We assumed that once in the intima the part of LDL is immediately oxidized. When the oxidized LDL exceeds a threshold, there is recruitment of monocytes. The incoming monocytes immediately differentiate into macrophages. Transformation of macrophages into foam cells contribute to the recruitment of new monocytes. It yields the secretion of a pro-inflammatory signal (cytokines), self-support inflammatory reaction. Newly formed foam cells are responsible for the local volume increase. Under a local incompressibility assumption, when foam cells are created the intima volume is locally increasing. Volume changing of the wall has influence on the fluid lumen domain which means that fully coupling is achieved. The specific numerical procedures with ALE formulation

were developed for this purpose. Our current approach is concentrated more on the process of plaque initiation and intimal thickening, rather than a huge plaque progression and rupture. We did not take into account smooth muscle cells proliferation in this model; this will be investigated in our future study.

We examined experimental data obtained for rabbit LDL transport model after few weeks of high fat diet, in order to determine material parameters of the computer model. From human carotid artery data, we investigated three time points for the carotid artery, zero, three and twelve months in order to make fitting of the model parameters for a specific patient, and two time points for coronary artery, zero and six months follow up. Three-dimensional reconstruction was performed from multi-CT scanner. Boundary conditions for the inlet velocity waveform were measured from Doppler ultrasound for coronary artery and from MRI for carotid artery. Shear stress distribution mostly corresponds to the localisation of the plaque volume progression. We matched animal data for plaque macrophages and volume progression for human data. Future research will go more into plaque structure for human data and additional different mechanisms for plaque progression.

Matching computed plaque location and progression in time with experimental observations demonstrates a potential benefit for future prediction of this vascular decease by using computer simulation.

Acknowledgments

This study was funded by a grant from FP7-ICT-2007 project (grant agreement 224297, ARTreat) and grants from Serbian Ministry of Education and Science III41007 and ON174028.

Извод

ARTREAT пројекат: компјутерска, експериментална и клиничка анализа тродимензионалног развоја и раста плака

Nenad Filipovic[1,2], Mirko Rosic[1], Velibor Isailovic[2], Zarko Milosevic[2], Dalibor Nikolic[2], Danko Milasinovic[2], Milos Radovic[2], Boban Stojanovic[1], Milos Ivanovic[1], Irena Tanaskovic[1], Igor Saveljic[2], Miljan Milosevic[2], Dejan Petrovic[2], Milica Obradovic[1], Exarchos Themis[3],Antonis Sakellarios[3], Panagiotis Siogkas[3], Paolo Marraccini[6], Federico Vozzi[6], Nicolas Meunier[4], Zhongzhao Teng[5], Dimitris Fotiadis[3],OberdanParodi[6], Milos Kojic[2,7]

[1]University of Kragujevac, Kragujevac, Serbia, fica@kg.ac.rs
[2]Metropolitan University Belgrade - R&D Center for Bioengineering, BioIRC, Serbia
[3]University of Ioannina, Ioannina, Greece
[4]University Paris Descartes, Paris, France
[5]University of Cambridge, Cambridge, Great Britain
[6]National Research Council Pisa, Italy
[7]The Methodist Hospital Research Institute, Houston, USA

Резиме

Атеросклероза је прогресивна болест коју карактерише инфламација, миграција моноцита-макрофага и акумулација липида у васкуларном зиду. Атеросклерозу иницијално карактерише ендотелна дисфункција, што појачава пролаз липидних и ћелијских елемената кроз крвни суд.

У овој студији смо истраживали тродимензиони компјутерски модел формирања и развоја плака који смо тестирали на експерименталним резултатима добијеним на зечевима и клиничким студијама на каротидним и коронарним артеријама код пацијената. Прво је симулиран модел транспорта LDL и формирања плака на животињским моделима зеца у оквиру једноставног експерименталног дизајна користећи хистолошке налазе. Онда су анализирани модели каротидних и коронарних артерија код појединих пацијената. Тродимензионално струјање крви је моделирано Навије-Стоксовим једначинама, заједно са једначином континуитета. Трансфер масе унутар домена струјања крви и кроз артеријски зид је спрегнут са струјањем крви и моделиран је конвективно-дифузионом једначином. Транспорт LDL у лумену крвног суда и кроз зид (што подразумева члан за губитак масе) је спрегнут са Кедем-Качалски једначинама. Инфламаторни процес је моделиран са три додатне реакционо-дифузионе једначине. Направљен је тродимензионални модел је који обједињује струјање крви, транспорт LDL и формирање и раст плака. Поредили смо запреминski раст плака користећи две и три тачке у времену, почетно, после 3 месеца и после 12 месеци стање за поједине каротидне артерије код пацијената. Такође је група пацијената са болешћу коронарних артерија анализирана на ангио уређајима компјутерском томографијом са циљем детектовања највеће акумулације LDL и повезивање са ниским смичућим напонима. Новина у овом раду је у систематској провери предвиђања раста плака који се прати са CTA 6 месеци после почетног стања код пацијената и где се специфични гранични услови за компјутерску симулацију задају са директних мерења појединих пацијената. Добијени резултати за позицију плака одговарају зонама ниских смичућих напона. Параметри модела су фитовани коришћењем нелинеарне методе најмањих квадрата. Разумевање и предвиђање развоја атеросклерозе било у стабилни или нестабилни плак су главни циљеви медицинске заједнице.

Кључне речи: атеросклероза, формирање и развој плака, компјутерско моделирање, метод коначних елемената, IVUS, хистологија

References

Libby, P., 2002, Inflammation in atherosclerosis, Nature, 868–874.

Loscalzo J., Schafer A. I., 2003. Thrombosis and Hemorrhage. Third edition. Lippincott Williams & Wilkins, Philadelphia.

Tarbell, J. M., 2003. Mass transport in arteries and the localization of atherosclerosis. Annual Review of Biomedical Engineering, 5, 79–118.

Zunino P., 2002. Mathematical and numerical modeling of mass transfer in the vascular system. PhD thesis, Lausanne, Switzerland: EPFL.

Quarteroni A., Veneziani A., Zunino P., 2002. Mathematical and numerical modeling of the solute dynamics in blood flow and arterial walls. SIAM Journal of Numerical Analysis, 39, 1488–1511.

Ross R., 1993. Atherosclerosis: a defense mechanism gone awry. Am J Pathol., 143, 987–1002.

Kedem, O., Katchalsky, A., 1961. A physical interpretation of the phenomenological coefficients of membrane permeability. The Journal of General Physiology, 45, 143–179.

Kedem, O., Katchalsky, A., 1958. Thermodynamic analysis of the permeability of biological membranes to non-electrolytes. Biochim. Biophys. 27, 229–246.

Kojic M., Filipovic N., Stojanovic B., Kojic N., 2008. Computer Modeling in Bioengineering: Theoretical Background, Examples and Software. John Wiley and Sons, Chichester, England.

Calvez V, AbderrhamanEbde, NicolasMeunier, AnnieRaoult, 2008. Mathematical modelling of the atherosclerotic plaque formation, ESAIM Proceedings, 28, 1-12.

Boynard M., Vincent Calvez, Ahmed Hamraoui, Nicolas Meunier, Annie Raoult, 2009. Mathematical modelling of earliest stage of atherosclerosis, COMPDYN 2009 - SEECCM 2009, Rhodes.

Filipovic, N., Meunier, N., Boynard, M., Kojic, M., Fotiadis, D., 2010. A 3D computer simulation of plaque formation and development in coronary artery, Proceedings of ASME 2010 First Global Congress on NanoEngineering for Medicine and Biology, NEMB2010, February 7-10, 2010 Houston, TX, USA.

Filipovic N., Mijailovic S., Tsuda A., Kojic M., 2006. An implicit algorithm within the Arbitrary Lagrangian-Eulerian formulation for solving incompressible fluid flow with large boundary motions, Comp. Meth. Appl. Mech. Eng., 195, 6347-6361.

Bourantas, C., Kourtis, I., Plissiti, M., Fotiadis, D., Katsouras, C., Papafaklis, M., Michalis, L., 2005, A Method for 3D reconstruction of coronary arteries using biplane angiography and intravascular ultrasound images, Comp. Med. Imag. Gr, 29, 597-606.

Bourantas, C., Kalatzis, F., Papafaklis, M., Fotiadis, D., Tweddel, A., Kourtis, I., Katsouras, C., Michalis, L., 2008, ANGIOCARE: An Automated System for Fast Three- Dimensional Coronary Reconstruction by Integrating Angiographic and Intracoronary Ultrasound Data, Cath. and Cardio. Interv., 72, 166 – 175.

Plissiti, M., Fotiadis, D., Michalis, L., Bozios, G., 2004, An Automated Method for Lumen and Media-Adventitia Border Detection in a Sequence of IVUS Frames," IEEE trans on Inf Tech. in Biomed,8, 131-141.

ARTreat FP7-224297 EU project 2008-2011. Multi-level patient-specific artery and atherogenesis model for outcome prediction, decision support treatment, and virtual hand-on training, www.artreat.org, www.artreat.kg.ac.rs.

Chavent, Guy, 2010. Nonlinear Least Squares for Inverse Problems, Nonlinear Least Squares for Inverse Problems Theoretical Foundations and Step-by-Step Guide for Applications, Springer, second print, New York.